North America's oldest boreal trees are more efficient water users due to increased [CO_2], but do not grow faster

Claudie Giguère-Croteau[a,b,c,1], Étienne Boucher[b,d,e,1,2], Yves Bergeron[a,c,f], Martin P. Girardin[g], Igor Drobyshev[c,f,h], Lucas C. R. Silva[i], Jean-François Hélie[b,j], and Michelle Garneau[b,d,e]

[a]Department of Biology, Université du Québec à Montréal, Montréal, QC H2X 1Y4, Canada; [b]GEOTOP, Université du Québec à Montréal, Montréal, QC H2X 1Y4, Canada; [c]Centre d'Études sur la Forêt, Université du Québec à Montréal, Montréal, QC H2X 1Y4, Canada; [d]Department of Geography, Université du Québec à Montréal, Montréal, QC H2X 3R9, Canada; [e]Centre d'Études Nordiques, Université Laval, Québec, QC G1V 0A6, Canada; [f]Institut de Recherche sur les Forêts, Université du Québec en Abitibi-Témiscamingue, Rouyn-Noranda, QC J9X 5E4, Canada; [g]Centre de Foresterie des Laurentides, Ressources Naturelles Canada, Sainte-Foy, QC G1V 4C7, Canada; [h]Swedish University of Agricultural Sciences, Southern Swedish Forest Research Centre, SE-230 53 Alnarp, Sweden; [i]Environmental Studies Program, Department of Geography, Institute of Ecology and Evolution, University of Oregon, Eugene, OR 97403; and [j]Department of Earth and Atmosphere Sciences, Université du Québec à Montréal, Montréal, QC H2X 3Y7, Canada

Edited by Donald R. Ort, University of Illinois, Urbana, IL, and approved December 20, 2018 (received for review September 27, 2018)

Due to anthropogenic emissions and changes in land use, trees are now exposed to atmospheric levels of [CO_2] that are unprecedented for 650,000 y [Lüthi et al. (2008) *Nature* 453:379–382] (thousands of tree generations). Trees are expected to acclimate by modulating leaf–gas exchanges and alter water use efficiency which may result in forest productivity changes. Here, we present evidence of one of the strongest, nonlinear, and unequivocal postindustrial increases in intrinsic water use efficiency (*iWUE*) ever documented (+59%). A dual-isotope tree-ring analysis ($\delta^{13}C$ and $\delta^{18}O$) covering 715 y of growth of North America's oldest boreal trees (*Thuja occidentalis* L.) revealed an unprecedented increase in *iWUE* that was directly linked to elevated assimilation rates of CO_2 (*A*). However, limited nutrient availability, changes in carbon allocation strategies, and changes in stomatal density may have offset stem growth benefits awarded by the increased *iWUE*. Our results demonstrate that even in scenarios where a positive CO_2 fertilization effect is observed, other mechanisms may prevent trees from assimilating and storing supplementary anthropogenic emissions as above-ground biomass. In such cases, the sink capacity of forests in response to changing atmospheric conditions might be overestimated.

water use efficiency | carbon dioxide | stable isotopes | productivity | boreal forest

Plants are an integral component of both water and carbon cycles on Earth. This is because stomata (i.e., microscopic apertures on plant leaves) allow plants to adjust their metabolism to changing environmental conditions by controlling the tradeoff between CO_2 intake for photosynthesis and water loss through transpiration. However, since the beginning of the industrial period, anthropogenic emissions and changes in land use resulted in a 40% increase in atmospheric [CO_2] (1) (hereafter referred to as c_a). Plants have not been exposed to concentrations above 290 ppm for at least 650,000 y (2, 3), so the dynamic carbon–water coupling that prevailed for several millennia could be disrupted with potential, yet uncertain, impacts on hydro-ecosystem functioning (4, 5).

One of the most striking consequences of elevated c_a is an increase in plant intrinsic water use efficiency (*iWUE*, i.e., the rate of carbon uptake per unit of water lost). The rate of increase of *iWUE* in response to rising c_a depends on how the assimilation rate (A) and/or stomatal conductance (g_s) adjusts to determine the optimal internal [CO_2] (c_i) (5, 6). Three theoretical scenarios (hereafter referred to as S1–S3) have been proposed (7) as guidelines on how to interpret possible acclimation strategies and their respective effects on *iWUE* (Fig. 1). In S1, plants maintain a constant c_i (*iWUE* increases strongly); in S2, there is a constant c_i/c_a ratio (*iWUE* increases moderately); and in S3, there is a constant difference between c_a and c_i (*iWUE* remains constant). Short-term flux measurements (4) and free-air CO_2 enrichment (FACE) experiments (8) have shown that S1 requires a strong and active physiological response leading to the highest rates of *iWUE* increase, most consistent with a strong CO_2 fertilization effect. However, the active *iWUE* response documented over short periods of time (yearly to decadal) may not reflect the changes occurring on longer timescales characteristic of natural forests (decadal to centennial). Over these timescales, there is no clear line of evidence that points toward a single, timescale-independent, acclimation strategy. To the contrary, the emerging concept of "optimal stomatal behavior" implies that woody plants shift along a continuum of strategies (5) and adjust g_s to maximize carbon gains while minimizing exposure to drought stress. This complex interplay takes place on yearly to multidecadal timescales and therefore requires the investigation of time series that are sufficiently long to be able to track and compare present-day stomatal behavior and *iWUE* changes to preindustrial reference levels.

Moreover, it is still unclear how these shifts in stomatal behavior impact forest productivity, i.e., whether changes in the rate of increase in *iWUE* are mirrored by changes in growth rates. Based on FACE studies (8), one could hypothesize that increases

Significance

The metabolism of North America's oldest boreal trees (*Thuja occidentalis* L.) is strongly affected by rising anthropogenic CO_2 emissions. Intrinsic water use efficiency (*iWUE*) increased dramatically, although nonlinearly, since the beginning of the industrial Era. Our study shows that while *T. occidentalis* L. acclimated to rising [CO_2], no stem growth was observed, suggesting that trees could not benefit from the increased *iWUE*.

Author contributions: C.G.-C., É.B., Y.B., I.D., and M.G. designed research; C.G.-C., É.B., and M.P.G. performed research; C.G.-C., É.B., M.P.G., and J.-F.H. contributed new reagents/analytic tools; C.G.-C., É.B., Y.B., M.P.G., I.D., L.C.R.S., and J.-F.H. analyzed data; C.G.-C., É.B., Y.B., M.P.G., I.D., L.C.R.S., and J.-F.H. wrote the paper; and É.B. provided funding.

The authors declare no conflict of interest.

This article is a PNAS Direct Submission.

[1]C.G.-C. and É.B. contributed equally to this work.

[2]To whom correspondence should be addressed. Email: boucher.etienne@uqam.ca.

This article contains supporting information online at www.pnas.org/lookup/suppl/doi:10.1073/pnas.1816686116/-/DCSupplemental.

Published online January 28, 2019.

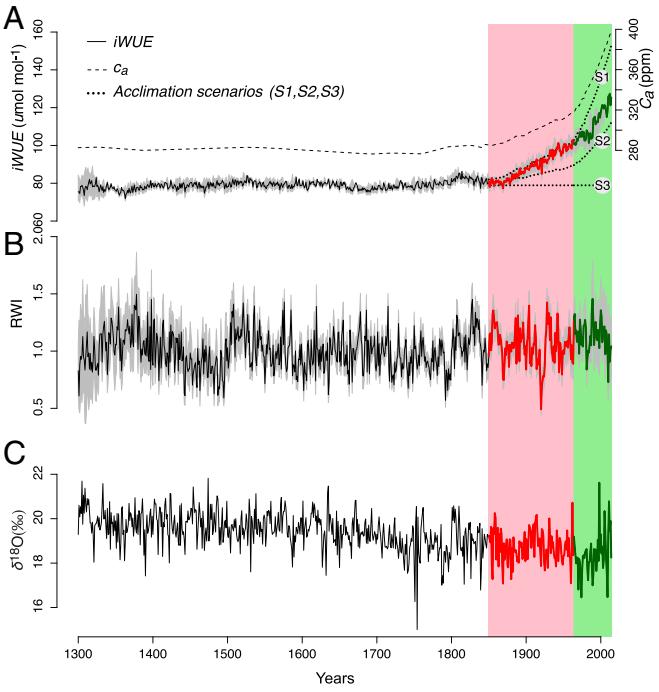

Fig. 1. Evolution of *iWUE*, c_a, RWI, and $\delta^{18}O$ since 1300 CE for old-growth white cedars at lake Duparquet, Eastern Canada. Two distinct periods emerge which have been highlighted through different coloring and shading: P1 (1850–1965, red) and P2 (1965–2014, green). (*A*) *iWUE* is calculated from $\delta^{13}C$-derived physiological parameters shown in Fig. 2. The gray shading around the *iWUE* curve represents the intertree variability. The three theoretical *iWUE* scenarios presented in the Introduction (S1, constant c_i; S2, constant c_i/c_a; and S3, constant $c_a - c_i$) are plotted as dotted lines. (*B*) Annually resolved RWI chronology, RCS standardized with bootstrap 95% CI (gray shading). (*C*) $\delta^{18}O$ values.

in *iWUE* (e.g., S1 or S2) would enhance stem growth. However, at least in boreal North America, tree-ring–based and bioclimatic modeling studies found little evidence of a widespread growth of forest stands that could be attributed to c_a increases (9, 10). Conversely, in this zone, growth has declined over vast portions of land, which has been attributed to the negative effects of temperature-induced droughts (10, 11). However, few of these tree-ring studies were accompanied by a thorough and time-continuous investigation of changes in gas exchange in response to increasing c_a. Only one study measured changes in *iWUE* and found that the positive response to c_a could not compensate for growth declines observed at the southernmost fringe of the boreal forest (12). Nevertheless, a high level of uncertainty persists with regard to the linkages between climate variability, *iWUE*, and forest productivity and their changes since preindustrial times.

To remedy this uncertainty, we report on the acclimation of a population of long-lived white cedars (*Thuja occidentalis* L.) growing in xeric conditions that offers a unique, long-term perspective on *iWUE*–growth relationships. We present a long (1300–2014), annually resolved, multiproxy tree-ring chronology in eastern North America (ring widths and stable isotopes of carbon and oxygen), to track changes in *iWUE* and growth attributable to rising c_a and climate variability for a period that extends far beyond the onset of the Industrial Era.

Results and Discussion

Acclimation to Rising c_a. Our results indicate a remarkable and unprecedented (59%) *iWUE* increase over the past 150 y (Fig. 1*A*). $\delta^{13}C$-derived physiological parameters reveal that old-growth white cedars have been acclimating to rising c_a in two distinct stages: period 1 (P1: 1850–1965, red shaded area in Fig. 1) and period 2 (P2: 1965–2014, green shaded area). During P1, a 37.42-ppm increase in c_a was accompanied by a slight and non-significant ($P > 0.05$) 1.84-ppm increase in c_i (Fig. 2 and *SI Appendix*, Table S1). This translates into a 28% *iWUE* increase compared with preindustrial (1300–1850) averages. Thus, during P1, for each increase of c_a of 1 ppm, c_i rose by only 0.05 ppm. This response nearly matches predictions from S1 according to which c_i would remain constant for increasing c_a (see Introduction for details) (Fig. 1*A*). Once c_a reached 320 ppm (onset of P2), c_i started to rise proportionally to c_a (Fig. 2), resulting in a constant c_i/c_a ratio of 0.49 (*SI Appendix*, Table S1), accompanied by an additional 31% increase in *iWUE* (in agreement with S2).

The observed rate of *iWUE* increase during P1 (0.59 $\mu mol \cdot mol^{-1}$ per ppm of c_a) is among the highest ever reported for the Northern Hemisphere (13–17). Thus, even at a mature age, white cedars can actively respond to rising c_a, by maintaining a constant c_i. Around the world, evidence from tree-ring analyses to support the hypothesis of a constant c_i (S1) exists, but is scarce. *Prosopis alba* (Griseb.) trees from the Atacama Desert (Chile) maintained a constant c_i from 1890 (earliest date in study) to 1980 (18). A population of Smith fir (*Abies georgei* var. smithii) trees of the southeastern Tibetan plateau in China (19) presented a constant c_i (150 ppm) from 1900 (earliest date in study) to 1944. In Finland, all beech, oak, and pine species also revealed a relatively constant c_i from 1895 (earliest date in study) to 1975 (20). At our site, once c_a reached 320 ppm, the rate of increase of *iWUE* slowed down to 0.31 $\mu mol \cdot mol^{-1}$ per 1 ppm of c_a, marking the beginning of P2 and a lower sensitivity to increasing c_a. While uncommon, similar shifts from a near-constant c_i to a proportional increase of c_i with rising c_a have been observed in relatively arid (19) and temperate areas (20), but were never reported in boreal North America.

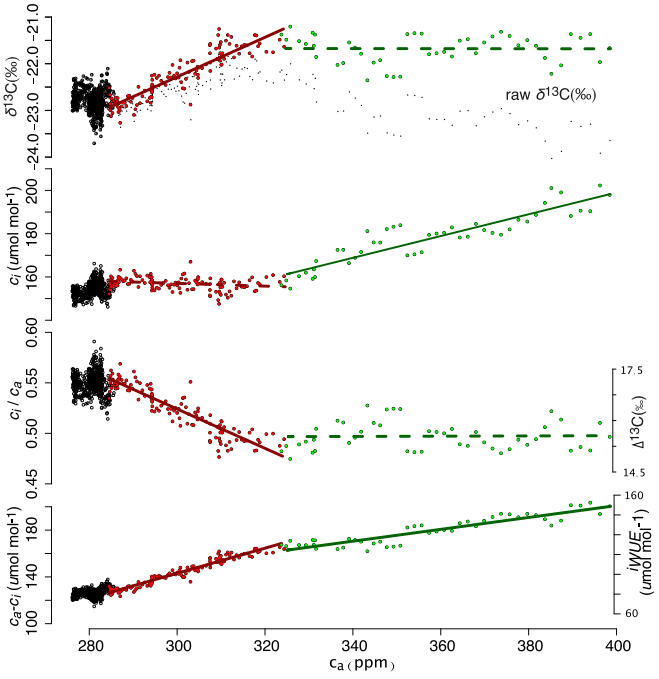

Fig. 2. Tree-ring $\delta^{13}C$ (corrected for Suess effect), derived physiological parameters ($\delta^{13}C$, c_i, c_i/c_a, Δ, $c_a - c_i$, *iWUE* plotted against c_a. The scatter plot is divided into three periods: preindustrial (black, <1850), P1 (red, 1850–1965), and P2 (green, 1965–2014). Linear trends describing the evolution of physiological parameters as a function of c_a are depicted for P1 and P2. Thick lines represent significant ($P < 0.05$) increasing or decreasing trends.

A shift in the acclimation strategy to rising c_a implies active physiological adjustments, either through carbon assimilation rate, A, or stomatal conductance, g_s, or both (5). To determine the relative importance of each factor for δ^{13}C-derived *iWUE* in white cedars, we used a tree-ring δ^{18}O analysis. According to the dual-isotope theory (21), the δ^{18}O composition of tree rings is unaffected by photosynthetic activity (22) and more influenced by source-water composition, isotopic exchanges with plant tissues, and evaporative enrichment of leaf water (23, 24). Our year-resolving tree-ring δ^{18}O time series (Fig. 1*C*) shows no correlation with δ^{13}C values ($P > 0.05$) and does not follow the increases in *iWUE* observed after 1850. Up to 1965, δ^{18}O remains relatively constant while δ^{13}C continually increases (*SI Appendix*, Fig. S11), suggesting that stimulation of A by increased CO_2 may be responsible for the pronounced increase in *iWUE* during P1. After 1965 (P2), however, mature *T. occidentalis* L. probably switched from an A-dominated to a g_s-dominated *iWUE* response. A steady increase in both δ^{18}O and *iWUE* which persists until the end of our time series indicates a declining stomatal conductance and transpiration, which is typically accompanied by enrichment in leaf water with ^{18}O due to the preferential evaporation of lighter oxygen isotopes (24).

Ultimately, our study provides in situ evidence of a shift in stomatal behavior: Old-growth white cedars maximized carbon gains at low c_a (during P1), but minimized water losses and exposure to drought stress at higher c_a (during P2). This switch in acclimation strategy is coherent with the one proposed by the optimal stomatal behavior theory (5). Indeed, based on a large number of field and $[CO_2]$-enrichment studies, the theory suggests that as c_a increases, no fixed homeostatic set point is observed in tree acclimation. Thus, at low c_a, plants seem to be profligate water users, as incremental increases in g_s lead to significant carbon gains. However, at high c_a, saturation of the photosynthetic apparatus forces the switch to a drought-avoidance strategy, because incremental increases in g_s lead to water losses that are disproportionately large relative to carbon gains. In conformity with that theory, we postulate that the shift from P1 to P2 indicates that white cedars are getting closer to saturation with rising c_a. *iWUE* of white cedars will thus continue to increase in the near future, but at half the pre-1965 rate.

Contributions of c_a and Climate to *iWUE* Variability. Commonality analysis revealed that both c_a and climate predictors [growing season (May–August) average air temperatures (T), soil moisture index (SMI), and vapor pressure deficit (VPD)] had a significant effect on *iWUE* during the 1953–2014 period. However, each variable had its maximal effect at a different time frequency. To show this, we incrementally filtered out the lower-frequency component of *iWUE*, each time computing a new commonality analysis (*Materials and Methods*). While the lower-frequency bands (f) between 0 cycle·y^{-1} and 0.03 cycle·y^{-1} (cycle lengths between ∞ and 75 y) were incrementally removed, c_a explained 75% ± 9% of the variance in *iWUE* and beta weights remained very high (0.9 ± 0.03) (Fig. 3 *A* and *B*). About 20% of the overall effect of c_a on *iWUE* also appeared to be shared with that of other climatic variables, namely VPD and T (Fig. 3 *C*, *1*). As the degradation of the *iWUE* signal continued, c_a quickly became less dominant and the importance of climate predictors progressively increased. For example, filtering out the low-frequency component of *iWUE* up to f = 0.05 cycle·y^{-1} (cycle lengths = 20 y) boosted beta weights and proportion of variance explained by climate predictors to a point that exceeds those of c_a (Fig. 3 *A* and *B*). More specifically, the pure (positive) effect of summer VPD at higher frequencies (cycle length = 20 y) rose to nearly 20% (±6%), while c_a had no more effect on *iWUE* at those timescales (Fig. 3 *C*, 2).

While most of the variance in *iWUE* can be explained by low-frequency variations in c_a, climate variables influence *iWUE* at the higher end of the frequency spectrum. The strong relationship between c_a and low-frequency changes in *iWUE* could somehow be expected because variations in *iWUE* are physiologically linked to c_a (25). At higher frequencies though, VPD, an important driver for transpiration, plays a slightly more important role in controlling *iWUE*, as documented for other species and environments (26). This implies that at annual to subdecadal timescales, increases in VPD led to reductions in stomatal conductance and increases in *iWUE* during the growing season (27).

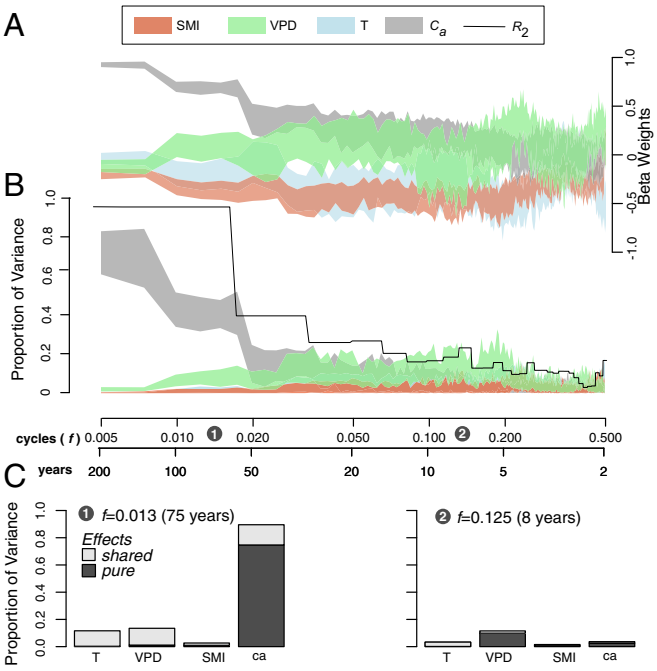

Fig. 3. (*A* and *B*) Commonality analysis showing beta weights (*A*) and the proportion of variance (*B*) in *iWUE* explained by the pure effects of c_a (gray) and growing-season (May–August) temperatures (T, blue), VPD (green), and SMI (red). Color bands represent the bootstrap 95% CIs for beta weights and proportion of variance explained in *iWUE*. (*C*) Pure and shared effects are detailed for two specific *iWUE* frequencies: f = 0.013 (75 y) (*C*, *1*) and f = 0.125 (8 y) (*C*, *2*).

The unprecedented increase in *iWUE* since 1850, however, cannot be attributed to changes in climate. For example, hypothesizing that the *iWUE* increase was climate induced would imply that increasingly dry conditions would have prevailed, causing a sustained stomatal closure and a drastic increase in *iWUE*. However, no such clear trend has been found in climate records extending back to 1901 (*SI Appendix*, Fig. S13). The pre-1965 period actually shows increasingly wetter/colder growing seasons (lower T and higher SMI). These pre-1965 trends seem to be confirmed by several independent dendrochronological indicators that point toward a decrease in the intensity and frequency of droughts in the area: The amount of biomass being burned in northwest Quebec has decreased since 1930 (28, 29), water levels of lake Duparquet have been rising since 1850 (30), and an increase in the severity of spring floods has been reported during that period (31). Growing-season climate conditions became drier/hotter only after 1965 (T increased, SMI decreased, and VPD increased).

As trees have been acclimating to rising c_a levels since the beginning of the Industrial Era, it appears plausible that climatic factors played only a marginal and indirect role in the observed interdecadal variability in *iWUE*. The strong stimulation of photosynthesis during P1 needed to rely upon a high stomatal conductance that probably would not have been possible if drier conditions prevailed. In contrast, the drier post-1965

climate conditions probably reinforced the drop in stomatal conductance during P2, therefore down-regulating photosynthesis and the rates of *iWUE* increase. In combination with the progressive saturation of the photosynthesis apparatus, this drying trend might represent an additional contributing factor that triggered the switch to a constant c_i/c_a (S2) acclimation strategy during P2.

No Unprecedented Growth Despite Increasing *iWUE*. Given the significant increase in *iWUE*, it appears reasonable to expect that white cedars experienced a substantially higher growth since 1850. However, our analysis of ring-width indexes (RWIs) shows that growth during the last 150 y was good, but not unprecedented at the scale of the last 715 y (Fig. 1*B*). Indeed, since 1300, at least three periods (early 1400s, 1520s, and mid-1800s) are equivalent in magnitude to the periods of high growth during the late 1980s–early 1990s.

Several studies have reported *iWUE* increases without apparent growth stimulation (13, 32–35). However, most of these studies found only modest average increases in *iWUE* (20% over the past 40 y) (32), reflecting a constant c_i/c_a adjustment (S2). Observed increases in growth that can be attributed to c_a (19) remain scarce and are inconsistently distributed across the Earth's biomes (32). The same holds for boreal Canada where only few measurements of *iWUE* are available and tree-ring widths provide little evidence for a positive growth trend that could be interpreted as a CO_2 –related stimulation of photosynthesis (9, 10, 13). White cedars typically found in mesic and hydric sites around Lake Duparquet even exhibited a notable growth decline during recent decades (36).

Four mechanisms can explain the lack of growth stimulation in a context of increasing *iWUE*. First, carbon allocation strategies might have shifted with time. Indeed, for slow-growing and water-stressed trees such as white cedars, priority in carbon allocation might be given to storage components other than the stem (which is used here as a proxy for growth). Under such conditions, a greater proportion of photosynthates would be used to produce volatile organic compounds or root exudates instead of above-ground biomass (37). Carbon taken up allocated to biosynthesis may also have been lowered owing to respiratory requirements for acquiring water and nutrients (38, 39). Second, the lack of growth stimulation in a context of increasing *iWUE* has often been associated to drought stress (13, 17, 33, 35). While we could not find any evidence for a persistent, century-long, drying trend (*SI Appendix*, Fig. S13), commonality analysis revealed that the RWI is positively (but poorly) related to the summer SMI (total effect <20%; *SI Appendix*, Fig. S11), implying that lateral growth could be limited when dry conditions prevail (40), especially during P2. Third, a progressive reduction in stomatal density (41) could also result in a rise of *iWUE* at the stomata scale without significant increase of total photosynthesis at the tree level. Higher CO_2 uptake by stomata co-occurring with a lower number of stomata would lead to carbon gains similar to the ones that prevailed during the preindustrial period. However, there should be a lower limit for stomatal density as scaled leaves need evaporative cooling and efficient CO_2 diffusion to the chloroplasts. Finally, nutrient limitation (42) also needs to be considered as a potential factor limiting growth in these thin-soiled, xeric environments. For example, in similar ecological conditions in southeastern Canada, ref. 43 found that phosphorus was the main limiting nutrient for slow-growing white cedars (apart from the limited physical space for root penetration in bedrock). An increase in leaf and root (but not trunk) biomass was observed in young white cedar saplings when supplied with additional phosphorus (43).

Our study has important implications for the modeling of vegetation response to atmospheric variability. Most ecophysiological and dynamic global vegetation models (DGVMs) predict an increase in plant biomass due to a stimulation of photosynthesis by c_a (44). Given the results presented here, such models might overestimate future forest carbon storage capacities. Our post-1850 data showed an unprecedented increase in *iWUE* that coincided with a drop in carbon use efficiency. These results imply that even when a marked stimulation of photosynthesis drove changes in *iWUE* (at least until 1965), the above-ground biomass did not increase substantially. Therefore, in light of previous findings (32), any assumption that positive stimulation of photosynthesis by CO_2 systematically translates into more carbon storage should be treated with caution. This result has wide-ranging implications for the modeling of climate–carbon feedbacks at the leaf–atmosphere interface and stresses the urgent need for additional research in this area to reduce these uncertainties.

Conclusions

North America's oldest boreal trees (*T. occidentalis* L.) exhibited an unprecedented 59% increase in *iWUE* since the beginning of the Industrial Era, mainly in response to rising atmospheric [CO_2] (c_a). This response was not constant in time, but a clear regime shift occurred around 1965, gradually switching the leaf gas-exchange strategy from a constant c_i to a constant c_i/c_a acclimation. Trees maximized carbon gains between 1850 and 1965 (P1) when the local climate was relatively wet and cold. Conversely, they reduced vulnerability to drought stress when the local climate became hotter and drier after 1965 (P2), possibly also combined with a closer saturation of the photosynthetic apparatus. However, the marked *iWUE* increase since 1850 did not translate into enhanced stem growth. This implies that other physiological processes such as nutrient availability, changes in carbon allocation strategies, or changes in stomatal density may have offset the growth benefits awarded by the increase in *iWUE*. Our results thus suggest that even in favorable conditions for growth, not all trees can take advantage of elevated levels of c_a and *iWUE*. These mechanisms are not typically taken into account by ecophysiological models (45) and DGVMs (44) which may lead to them overestimating any positive effects bestowed by a higher c_a on carbon assimilation and fixation. Predictions of elevated future growth and possible alleviating effects on c_a might be overly optimistic if the models do not allow for the possibility of constant or even reduced growth in the context of increasing c_a. It would be advisable to define improved allocation rules and determine whether those rules can change over time (and with increasing c_a). Integrating measurements acquired at shorter time intervals (daily or weekly resolution) with long times series of tree-ring measurements would further help to track and define those allocation rules in trees exposed to a varying climate and nutrient availability.

***SI Appendix*.** *SI Appendix* provides complementary information on methods and results: the regional curve used for regional curve standardization (RCS), quality statistics for the RCS chronology, cohorts selected for $\delta^{13}C$ and $\delta^{18}O$ analysis and their junction, effect of correction methods on $\delta^{13}C$ chronology, and results for whole-wood and cellulose $\delta^{13}C$ and $\delta^{18}O$ values comparison.

Materials and Methods

Study Site and Sampling Strategy. Lake Duparquet is located at the southern limit of the boreal forest (48,47° N, 79,27° W), in northeastern Canada (*SI Appendix*, Fig. S1). Climate is continental, cold, and humid, with a mean annual temperature of 1 °C and a mean annual total precipitation of 985.2 mm (climate normals for 1981–2010 from Station Mont-Brun, located 12 km south and 42 km east from Duparquet) (46). In 1987, 39 trees were sampled by ref. 40. To extend their ring-width chronology (1186–1987) until 2014, 35 trees, spread across five islands and six peninsulas of Lake Duparquet (*SI Appendix*, Fig. S1), were resampled in 2012 and 2014 using a 5-mm core increment borer at chest height. Sixteen trees were also part of the

first chronology by ref. 40. Trees were measured, cross-dated, and detrended using the RCS approach (47) (*SI Appendix*).

Stable Isotope Chronologies. Eleven trees were selected for carbon and oxygen stable isotope ratio analysis to cover the maximum time period with the smallest number of possible cohort changes (*SI Appendix*, Fig. S4). This avoids loss of a reliable mean as we go back in time, considering the systematic offsets typically encountered in the stable isotope analyses of different trees (25, 48, 49). Isotope chronologies have been shown to require few replicates (as little as four) to obtain a strong common signal (expressed population signal $\geq$0.85) (25). Two cohorts of six (cohort 1: 1620–2014) and five trees (cohort 2: 1295–1645) were selected, with an overlap of 25 y (*SI Appendix*, Fig. S4). The trees selected for stable isotope analysis had different ages that were well spread through time. This avoids incorporating noise due to nonclimatic age effects (*SI Appendix*, Fig. S4). The first 50 y of each sample were excluded to avoid any nonclimatic age-related trends (49, 50) (*SI Appendix*).

δ^{13}C-Derived Physiological Parameters. $\delta^{13}C$ variability in tree rings depends on processes by which trees fractionate carbon at the leaf gas-exchange site (discrimination against ^{13}C vs. ^{12}C) before fixing it in the stem during the growing season (25, 51). Carbon fractionation (Δ, ‰) is expressed as the difference between $\delta^{13}C$ values of atmospheric CO_2 ($\delta^{13}C_{air}$) and tree-ring $\delta^{13}C$ values ($\delta^{13}C_{tree}$) as shown by Eq. **1** (7):

$$\Delta(‰) = \frac{\delta^{13}C_{air} - \delta^{13}C_{tree}}{1 + \delta^{13}C_{tree}/1{,}000} \approx \delta^{13}C_{air} - \delta^{13}C_{tree}. \quad [1]$$

Carbon fractionation thus occurs in two main steps (52): CO_2 diffusion through stomata (step $i \approx -4.4‰$; ref. 53) and carboxylation (step $ii \approx -27‰$; refs. 25 and 54). However, the overall fractionation is dependent on the ratio between leaf intercellular (c_i) and ambient (c_a) CO_2 concentrations:

$$\Delta \approx \delta^{13}C_{air} - \delta^{13}C_{tree} = a + (b - a)\frac{c_i}{c_a}. \quad [2]$$

Records of $\delta^{13}C_{air}$ and c_a obtained from Antarctic ice cores by ref. 55 were linearly interpolated until 1295. From 1850 to 2003, values from ref. 25 were used (following refs. 2, 4, and 55) and linearly interpolated until 2014.

Based on plant physiology theory and models, physiological parameters can be derived from tree-ring $\delta^{13}C$ values. c_i is calculated from Eq. **2**, provided that all other variables are known. *iWUE*, a measure of the amount of carbon assimilated per unit leaf area per unit time per unit cost of water, is calculated as (18)

$$iWUE = \frac{A}{g_s} = \frac{c_a - c_i}{1.6}. \quad [3]$$

According to Eq. **3**, the difference between c_a and c_i is proportional to *iWUE* and reflects the balance between the rate of CO_2 assimilation (A) and stomatal conductance (g_s).

For each of the three theoretical scenarios of leaf–gas strategy (7), the $\delta^{13}C$ response to c_a is shown in Fig. 2 (main text). This was achieved by fixing c_i accordingly, using Eq. **3**. Scenarios start in 1850, at the beginning of the industrial period, and exhibit a linear response to c_a increases and assume a negligible c_i response to climate variability. The c_i preindustrial level was 150 ppm (the 1295–1850 mean).

Dendroclimatic Analyses. Daily weather data (1901–2014 maximum and minimum temperatures) and precipitation (1901–2014 sum) and VPD (1953–2014) were retrieved from BioSIM v.10, which interpolates site-specific estimates from historical weather observations (56) as described in ref. 57. The quantity of available soil moisture was estimated for each month using the quadratic + linear (QL) formulation procedure described in ref. 58, which accounts for water loss through evapotranspiration (simplified Penman–Monteith potential evapotranspiration) and gain from precipitation. Parameter values for maximum and critical available soil water were set at 300 mm and 400 mm, respectively; the number of weather stations for interpolation was set to eight. We used values of annual mean c_a recorded at Mauna Loa observatory since 1958 (59); the data were extended to 1901 using estimates from ice cores (60).

Commonality analysis (61) was used to explore the climate effects of c_a and climate predictors on *iWUE*, $\delta^{18}O$, and RWI. With a commonality analysis, one seeks to decompose linear regression R_2 into its unique and common effects. Unique effects indicate how much variance is uniquely accounted for by a single variable, taken as a single predictor. Common effects indicate how much variance is common to a set of predictors. Total effects refer to the combination of unique and common effects and describe the explanatory power of a predictor, summing up all commonalities. Commonality analysis is particularly useful to estimate effects in the presence of multicollinearity in a predictor dataset. For each analysis, we show regression beta weights, unique effects, common effects, and total effects for each variable, as well as R_2 values for the whole regression model. For simplicity, we chose to use a limited set of predictor variables: May–August (growing season) temperatures (T), SMIs, and VPDs. We performed the commonality analysis iteratively; i.e., the data were passed several times through a high-pass filter which led to incremental degradation of the original *iWUE* variable, as each pass removed a bigger part of the low frequencies. Hence, at the beginning of the loop *iWUE* contained all frequencies from $0 \leq f \leq 0.5\ y^{-1}$ (cycle lengths between ∞ and 2 y) while at the end of the iteration *iWUE* was degraded to a perfectly detrended seesaw signal with $f = 0.5\ y^{-1}$ (cycle length = 2 y). The iterative degradation of the original *iWUE* signal coupled to the commonality analysis allowed us to pinpoint those frequencies above or below which c_a and climate had a dominant influence on *iWUE*, $\delta^{18}O$, and RWI.

ACKNOWLEDGMENTS. We acknowledge the contribution of many people who helped with field and laboratory work: A. Barbe, G. Proulx, P. Leclerc, M. Gratton, and A. Adamowicz-Walczak. We thank the Natural Sciences and Engineering Research Council (NSERC) and Her Majesty The Queen in due right of Canada. C.G.-C. acknowledges financial support from both NSERC and Fonds de Recherche Québécois Nature et Technologies for her master's thesis.

1. Robertson A, et al. (2001) Hypothesized climate forcing time series for the last 500 years. *J Geophys Res Atmos* 106:14783–14803.
2. Lüthi D, et al. (2008) High-resolution carbon dioxide concentration record 650,000–800,000 years before present. *Nature* 453:379–382.
3. Petit JR, et al. (1999) Climate and atmospheric history of the past 420,000 years from the Vostok ice core, Antarctica. *Nature* 399:429–436.
4. Keenan TF, et al. (2013) Increase in forest water-use efficiency as atmospheric carbon dioxide concentrations rise. *Nature* 499:324–327.
5. Voelker SL, et al. (2016) A dynamic leaf gas-exchange strategy is conserved in woody plants under changing ambient CO2: Evidence from carbon isotope discrimination in paleo and CO2 enrichment studies. *Glob Change Biol* 22:889–902.
6. Ehleringer JR, Cerling TE (1995) Atmospheric CO2 and the ratio of intercellular to ambient CO2 concentrations in plants. *Tree Physiol* 15:105–111.
7. Saurer M, Siegwolf RT, Schweingruber FH (2004) Carbon isotope discrimination indicates improving water-use efficiency of trees in northern Eurasia over the last 100 years. *Glob Change Biol* 10:2109–2120.
8. Battipaglia G, et al. (2013) Elevated CO2 increases tree-level intrinsic water use efficiency: Insights from carbon and oxygen isotope analyses in tree rings across three forest face sites. *New Phytol* 197:544–554.
9. Gedalof Z, Berg AA (2010) Tree ring evidence for limited direct CO2 fertilization of forests over the 20th century. *Glob Biogeochem Cycles* 24:GB3027.
10. Girardin MP, et al. (2016) No growth stimulation of Canada's boreal forest under half-century of combined warming and CO2 fertilization. *Proc Natl Acad Sci USA* 113:E8406–E8414.
11. Girardin MP, et al. (2016) Negative impacts of high temperatures on growth of black spruce forests intensify with the anticipated climate warming. *Glob Change Biol* 22:627–643.
12. Silva LC, Anand M, Leithead MD (2010) Recent widespread tree growth decline despite increasing atmospheric CO2. *PloS one* 5:e11543.
13. Silva LC, Horwath WR (2013) Explaining global increases in water use efficiency: Why have we overestimated responses to rising atmospheric CO2 in natural forest ecosystems? *PLoS One* 8:e53089.
14. Frank D, et al. (2015) Water-use efficiency and transpiration across European forests during the Anthropocene. *Nat Clim Change* 5:579–583.
15. Brienen RJ, Lebrija-Trejos E, Zuidema P, Martinez-Ramos M (2010) Climate-growth analysis for a Mexican dry forest tree shows strong impact of sea surface temperatures and predicts future growth declines. *Glob Change Biol* 16:2001–2012.
16. Gómez-Guerrero A, et al. (2013) Growth decline and divergent tree ring isotopic composition (δ13C and δ18O) contradict predictions of CO2 stimulation in high altitudinal forests. *Glob Change Biol* 19:1748–1758.
17. Saurer M, et al. (2014) Spatial variability and temporal trends in water-use efficiency of European forests. *Glob Change Biol* 20:3700–3712.
18. Ehleringer JR (1993) Carbon and water relations in desert plants: An isotopic perspective. *Stable Isotopes and Plant Carbon-Water Relations*, eds Ehleringer JR, Hall AE, Farquhar GD (Elsevier, San Diego), pp 155–172.
19. Huang R, et al. (2017) Does increasing intrinsic water use efficiency (iWUE) stimulate tree growth at natural alpine timberline on the southeastern Tibetan plateau? *Glob Planet Change* 148:217–226.

20. Waterhouse JS, et al. (2004) Northern European trees show a progressively diminishing response to increasing atmospheric carbon dioxide concentrations. *Quat Sci Rev* 23:803–810.
21. Scheidegger Y, Saurer M, Bahn M, Siegwolf R (2000) Linking stable oxygen and carbon isotopes with stomatal conductance and photosynthetic capacity: A conceptual model. *Oecologia* 125:350–357.
22. Yakir D (1992) Variations in the natural abundance of oxygen-18 and deuterium in plant carbohydrates. *Plant Cell Environ* 15:1005–1020.
23. Roden JS, Ehleringer JR (1999) Hydrogen and oxygen isotope ratios of tree-ring cellulose for riparian trees grown long-term under hydroponically controlled environments. *Oecologia* 121:467–477.
24. Barbour MM (2007) Stable oxygen isotope composition of plant tissue: A review. *Funct Plant Biol* 34:83–94.
25. McCarroll D, Loader NJ (2004) Stable isotopes in tree rings. *Quat Sci Rev* 23:771–801.
26. Maxwell TM, Silva LCR, Horwath WR (2018) Integrating effects of species composition and soil properties to predict shifts in montane forest carbon–water relations. *Proc Natl Acad Sci USA* 115:E4219-E4226.
27. Farquhar GD, Sharkey TD (1982) Stomatal conductance and photosynthesis. *Annu Rev Plant Physiol* 33:317–345.
28. Girardin MP, et al. (2013) Fire in managed forests of eastern Canada: Risks and options. *For Ecol Manage* 294:238–249.
29. Drobyshev I, et al. (2017) Strong gradients in forest sensitivity to climate change revealed by dynamics of forest fire cycles in the post Little Ice Age era. *J Geophys Res Biogeosci* 122:2605–2616.
30. Denneler B, Asselin H, Bergeron Y, Begin Y (2008) Decreased fire frequency and increased water levels affect riparian forest dynamics in southwestern boreal Quebec, Canada. *Can J For Res* 38:1083–1094.
31. Tardif J, Bergeron Y (1997) Ice-flood history reconstructed with tree-rings from the southern boreal forest limit, western Québec. *Holocene* 7:291–300.
32. Peñuelas J, Canadell JG, Ogaya R (2011) Increased water-use efficiency during the 20th century did not translate into enhanced tree growth. *Glob Ecol Biogeogr* 20:597–608.
33. Dietrich R, et al. (2016) Climatic sensitivity, water-use efficiency, and growth decline in boreal jack pine (Pinus banksiana) forests in Northern Ontario. *J Geophys Res Biogeosci* 121:2761–2774.
34. Lévesque M, Siegwolf R, Saurer M, Eilmann B, Rigling A (2014) Increased water-use efficiency does not lead to enhanced tree growth under xeric and mesic conditions. *New Phytol* 203:94–109.
35. Andreu-Hayles L, et al. (2011) Long tree-ring chronologies reveal 20th century increases in water-use efficiency but no enhancement of tree growth at five Iberian pine forests. *Glob Change Biol* 17:2095–2112.
36. Housset JM, Girardin MP, Baconnet M, Carcaillet C, Bergeron Y (2015) Unexpected warming-induced growth decline in Thuja occidentalis at its northern limits in North America. *J Biogeogr* 42:1233–1245.
37. Vicca S, et al. (2012) Fertile forests produce biomass more efficiently. *Ecol Lett* 15:520–526.
38. Manzoni S, et al. (2018) Reviews and syntheses: Carbon use efficiency from organisms to ecosystems–definitions, theories, and empirical evidence. *Biogeosciences* 15:5929–5949.
39. Delucia E, Drake J, Thomas R, Gonzalez-Meler M (2007) Forest carbon use efficiency: Is respiration a constant fraction of gross primary production? *Glob Change Biol* 13:1157–1167.
40. Archambault S, Bergeron Y (1992) An 802-year tree-ring chronology from the Quebec boreal forest. *Can J For Res* 22:674–682.
41. Lake J, Quick W, Beerling DJ, Woodward FI (2001) Plant development: Signals from mature to new leaves. *Nature* 411:154.
42. Norby RJ, Warren JM, Iversen CM, Medlyn BE, McMurtrie RE (2010) CO2 enhancement of forest productivity constrained by limited nitrogen availability. *Proc Natl Acad Sci USA* 107:19368–19373.
43. Matthes-Sears U, Nash CH, Larson DW (1995) Constrained growth of trees in a hostile environment: The role of water and nutrient availability for Thuja occidentalis on cliff faces. *Int J Plant Sci* 156:311–319.
44. Sitch S, et al. (2008) Evaluation of the terrestrial carbon cycle, future plant geography and climate-carbon cycle feedbacks using five dynamic global vegetation models (DGVMs). *Glob Change Biol* 14:2015–2039.
45. Guiot J, Boucher E, Gea-Izquierdo G (2014) Process models and model-data fusion in dendroecology. *Front Ecol Evol* 2:52.
46. Government of Canada (2016) Canadian climate normals 1981-2010. Available at climate.weather.gc.ca/climate_normals/index_e.html. Accessed April 25, 2017.
47. Esper J, Cook ER, Krusic PJ, Peters K, Schweingruber FH (2003) Tests of the RCS method for preserving low-frequency variability in long tree-ring chronologies. *Tree Ring Res* 59:81–98.
48. Gagen M, et al. (2012) A rapid method for the production of robust millennial length stable isotope tree ring series for climate reconstruction. *Glob Planet Change* 82:96–103.
49. Labuhn I, et al. (2014) Tree age, site and climate controls on tree ring cellulose δ18O: A case study on oak trees from south-western France. *Dendrochronologia* 32:78–89.
50. Young GH, et al. (2011) Age trends in tree ring growth and isotopic archives: A case study of Pinus sylvestris L. from northwestern Norway. *Glob Biogeochem Cycles* 25:GB2020.
51. Gessler A, et al. (2014) Stable isotopes in tree rings: Towards a mechanistic understanding of isotope fractionation and mixing processes from the leaves to the wood. *Tree Physiol* 34:796–818.
52. Farquhar GD, O'Leary MH, Berry JA (1982) On the relationship between carbon isotope discrimination and the intercellular carbon dioxide concentration in leaves. *Funct Plant Biol* 9:121–137.
53. O'Leary MH (1981) Carbon isotope fractionation in plants. *Phytochemistry* 20:553–567.
54. Farquhar G, Richards R (1984) Isotopic composition of plant carbon correlates with water-use efficiency of wheat genotypes. *Funct Plant Biol* 11:539–552.
55. Francey R, et al. (1999) A 1000-year high precision record of δ13C in atmospheric CO2. *Tellus B* 51:170–193.
56. Environment Canada (2013) National climate data and information archive. Available at climate.weatheroffice.gc.ca/. Accessed April 25, 2017.
57. Régnière J, Bolstad P (1994) Statistical simulation of daily air temperature patterns eastern North America to forecast seasonal events in insect pest management. *Environ Entomol* 23:1368–1380.
58. Hogg E, Barr A, Black T (2013) A simple soil moisture index for representing multi-year drought impacts on aspen productivity in the western Canadian interior. *Agric For Meteorol* 178:173–182.
59. Keeling CD, et al. (2001) Exchanges of atmospheric CO2 and 13CO2 with the terrestrial biosphere and oceans from 1978 to 2000: I. Global aspects (Scripps Institution of Oceanography, San Diego), SIO Reference Series, No. 01-06.
60. Etheridge DM, et al. (1996) Natural and anthropogenic changes in atmospheric CO2 over the last 1000 years from air in Antarctic ice and firn. *J Geophys Res Atmos* 101:4115–4128.
61. Ray-Mukherjee J, et al. (2014) Using commonality analysis in multiple regressions: A tool to decompose regression effects in the face of multicollinearity. *Methods Ecol Evol* 5:320–328.